Philippine Journal of Science
154 No. (1): 73-82, February 2025
ISSN 0031 - 7683
Date Received: 16 Jul 2024

DNA Aptamer Selection against *Mycobacterium tuberculosis* Antigen 85 Complex Using Microplate-based SELEX

Resmond L. Reaño[1]*, Clydee Ann T. Hernandez[1], Jeffrey P. Tamayo[2], and Christian Adam L. Espiritu[3,4]

[1]Department of Engineering Science, College of Engineering and Agro-industrial Technology, University of the Philippines Los Baños, Los Baños, Laguna 4031 the Philippines
[2]Central Analytical Services Laboratory, National Institute of Molecular Biology and Biotechnology, University of the Philippines Los Baños, Los Baños, Laguna 4031 the Philippines
[3]College of Medicine, University of Northern Philippines, Vigan City, Ilocos Sur 2700 the Philippines
[4]Center for Research and Development, Davao Medical School Foundation, Inc., Davao City 8000 the Philippines

Antigen 85 complex (Ag85c) secreted by *Mycobacterium tuberculosis* is a promising TB biomarker due to its abundance in the blood sera of active TB patients. This study aimed to identify an aptamer against Ag85c antigen using a microplate-based protein-SELEX process. The study also aimed to determine the enriched sequence *via* capillary electrophoresis sequencing and perform binding affinity and cross-reactivity study using direct enzyme-linked oligonucleotide assay. The binding kinetics of the successful aptamer was further studied using surface plasmon resonance (SPR). The aptamer sequence was identified by capillary electrophoresis sequencing and denoted as H1. Aptamer H1 has a strong affinity with apparent K_d (based on EC_{50} obtained *via* ELONA) equal to 0.00272 nM and specificity to the target Ag85c compared with a non-specific aptamer, H2 with apparent K_d (EC_{50}) of 0.383 nM. SPR showed a strong binding affinity of 20.93 nM (U-value = 12) between aptamer H1 and the target antigen TB Ag85c. The results showed that aptamer H1 has a strong potential as a bio-probe for developing bioassays and biosensors for TB diagnostics.

Keywords: antigen 85 complex, DNA aptamer, *Mycobacterium tuberculosis*, surface plasmon resonance, TB antigen

INTRODUCTION

Tuberculosis (TB) remains a significant public health concern and the most common cause of death among adults from infectious diseases (Barbier *et al*. 2023). TB is caused by the bacteria *Mycobacterium tuberculosis* (*M. tb.*), an ancient pathogen that has been persistent due to its complex survival strategies in the living host and the environment. It has developed a repertoire of culture filtrate antigens that multiply as the disease progresses (Samanich *et al*. 2000; Tucci *et al*. 2020). Rapid, sensitive, easy-to-use, inexpensive, and portable TB diagnostics are essential in controlling and preventing this disease (Barbier *et al*. 2023). Among the prominent and readily available approaches is

*Corresponding author: rlreano@up.edu.ph

detecting those antigens secreted by *M. tb.* (Bekmurzayeva *et al*. 2013). Among the notable TB antigens and biomarkers are Mpt-64, Ag85 complex, CFP10, ESAT6, LAM, HBHA, HspX, and LpqH, which can be detected using serologic immunoassay (Krishnananthasivam *et al*. 2023; Bekmurzayeva *et al*. 2013).

The antigen 85 complex (Ag85c) has been popular for developing TB diagnostics due to its abundance in blood circulation as *M. tb.* replicates or as the infection progresses (Barbier *et al*. 2023; Phunpae *et al*. 2014). The 30-32 kDa Ag85c is a family of three proteins present at a ratio of 2:3:1 (Ag85A @ 32 kDa, Ag85B @ 30 kDa, and Ag85C @32.5 kDa). It is an immunodominant mycobacterial antigen and among the most promising TB vaccine candidate antigens (Huygen 2014; Ansari *et al*. 2018). It was determined that blood circulating levels of Ag85c are elevated in patients with active TB. The median serum Ag85c level of TB-infected patients was found to be 50–150 times higher than those with active non-tuberculous pulmonary disease or healthy controls. There was no increase in Ag85c using urine samples despite the high levels in blood serum. Ag85c exists in the blood as complexes with immunoglobins and plasma proteins, accounting for its lack of urinary clearance (Bentley-Hibbert *et al*. 1999). Reports have shown various techniques for Ag85c detection such as conventional ELISA, immunoblotting, direct liquid chromatography-tandem mass spectroscopy, and waveguide-based optical biosensors (Barbier *et al*. 2023).

Despite its popularity, ELISA exhibits some drawbacks such as batch-to-batch result inconsistencies, the expensive and time-consuming process of antibody production, and the unstable nature of antibodies during storage and transport. Enzyme-linked oligonucleotide assay (ELONA) was developed akin to ELISA, replacing the antibody with aptamers for the target biomolecule recognition (Shola David and Kanayeva 2022). Aptamers gained research interest since it was revealed in 1990 as a potential rival to antibodies in terms of their diverse application due to their ability to form 2D and 3D shapes that help them to recognize and bind to their cognate target with high affinity and specificity (Jayasena 1999). Aptamers are short single-stranded nucleic acids (can be DNA or RNA) that are selected from a set of random oligonucleotide libraries and synthesized *in vitro* using a method called systematic evolution of ligands by exponential enrichment (SELEX) (Sypabekova *et al*. 2017; Ansari *et al*. 2018). In contrast to antibodies, aptamers are more stable in complex environments and highly resistant to denaturation and degradation when modified and optimized appropriately. Aptamers can be synthesized chemically, allowing easy incorporation of functional groups suitable for a particular type of application. This also allows more straightforward labeling of aptamers with electroactive or electrocatalytic compounds to support redox reactions for electrochemical applications (Bezerra *et al*. 2019; McKeague *et al*. 2022; Ansari *et al*. 2018; Reaño and Escobar 2024).

Aptamers can be exploited to develop a biosensor due to their high affinity and specificity to a target molecule. Aptamers are synthetic nucleic acid strands or oligonucleotides that can be immobilized on the transducer's surface. A biosensor using aptamers as recognition material is referred to as an aptasensor. Aptamers are versatile and can show conformational changes upon binding with a target molecule. This property makes them the most suitable and appropriate candidate for designing a miniaturized and portable analytical device. Small-sized target molecules can be enfolded inside the aptamer as it folds itself, whereas folded aptamer can bind to large molecules such as proteins, inducing conformational change. Therefore, an aptasensor can be fabricated using any aptamer that responds to a specific ligand. Despite its notable advantages, reports on applying aptamers in TB diagnostics are still scarce (Ansari *et al*. 2018; Espiritu *et al.* 2018; Reaño and Escobar 2024).

This study aimed to isolate aptamers with high binding affinity and specificity to the *M. tb.* antigen Ag85c using a microplate-based SELEX process and identify the isolated sequences by capillary electrophoresis sequencing. It also aimed to validate the binding affinity of the aptamer using ELONA and surface plasmon resonance (SPR) for possible use in TB diagnostic.

MATERIALS AND METHODS

Materials

The Ag85c – composed of fibronectin-binding proteins FbpA, FbpB, and FbpC – purified native protein from *M. tb.* Strain H37Rv, the 30 kDa recombinant form of the antigen 85 complex A (Ag85A) protein, the 11 kDa recombinant form of the early secretory antigenic target protein (ESAT-6), and the 19 kDa recombinant and conserved form of lipoprotein antigen precursor (LpqH) from *M. tb*. were all obtained through BEI Resources, National Institute of Allergy and Infectious Diseases (NIAID), National Institutes of Health (NIH) (Rockville, MD, USA). The desalted primers, oligonucleotide library, and biotinylated aptamers were purchased from Integrated DNA Technologies (Singapore).

For ELONA the following reagents were used: horseradish peroxidase (HRP) conjugated to streptavidin (ABCAM, CAM, UK), 3,3',5,5'-tetramethylbenzidine (TMB)

(Promega, WI, USA), PBS in powdered form (10-mM phosphate, 138-mM NaCl, and 2.7-mM KCl at pH 7.4) (Sigma-Aldrich, MA, USA), and tween 20 (for 0.05% v/v PBS-tween buffer at pH 7.4) (Promega, WI, USA).

All polymerase chain reaction (PCR) reagents were purchased from Thermo Fischer Scientific (MA, USA), whereas the oligonucleotide purification kits were purchased from Zymo Research (CA, USA). All salts, acids, and bases used were ACS grade and purchased from JT Baker (NJ, USA) and Merck (MA, USA). All solutions were prepared using biotechnology-grade nuclease-free, purified, and sterilized ultrapure water, using 1-µm membrane filtration and autoclaving.

Microplate-based Systematic Evolution of Ligands by Exponential Enrichment (p-SELEX)

The p-SELEX process developed by Espiritu *et. al.* (2018) was adopted in this study and is illustrated in Figure 1A. In a 96-well microtiter plate, 50 µL (at 50 µg/mL) of PBS (negative SELEX), LpqH (counter SELEX 1), ESAT-6 (counter SELEX 2), and Ag85c (positive SELEX) antigens were separately immobilized in A1, C1, E1, and G1 respectively for the first SELEX round, wells of Costar® high binding polystyrene assay plate (Corning, Inc., NY, USA), for 1 h at 37 °C. The fluids in the wells were then removed, and 200 µL of PBS-Tween 20 was added and incubated for 30 min at 37 °C. After the blocking step, the wells were washed thrice with 200 µL of PBS-Tween 20, followed by the incubation of 100 µL of the oligonucleotide library dissolved in SELEX buffer (PBS with 2.5 mM $MgCl_2$, pH 6.4) for 30 min in the PBS containing well at 37 °C. The original oligonucleotide library contains about 10^{15} single-stranded DNA, prepared by diluting 3 µL (of the 100 µM) of the random oligonucleotide to 100 µL with the SELEX buffer. The bound oligonucleotides were recovered and amplified for the succeeding rounds based on the desired concentration determined by comparing the agarose gel bands.

The unbound aptamer pool was then transferred to the well where the counter-target, ESAT-6 antigen, was immobilized and incubated for 30 min at 37 °C. The procedure was repeated using the LpqH antigen before transferring it to the Ag85c-containing well and incubating it under the same conditions. After incubation, the fluid was removed, and the well was washed thrice with 200 µL of SELEX buffer. The resulting oligonucleotide pool was eluted using 30 µL of ultrapure water at 95 °C and was stored at –20 °C. The eluted oligonucleotide pool was amplified to double-stranded DNA *via* the PCR technique. The number of PCR cycles was determined by comparing the agarose gel electrophoresis results with a standard. The single-stranded DNA for the next round was prepared from the amplified double-stranded DNA

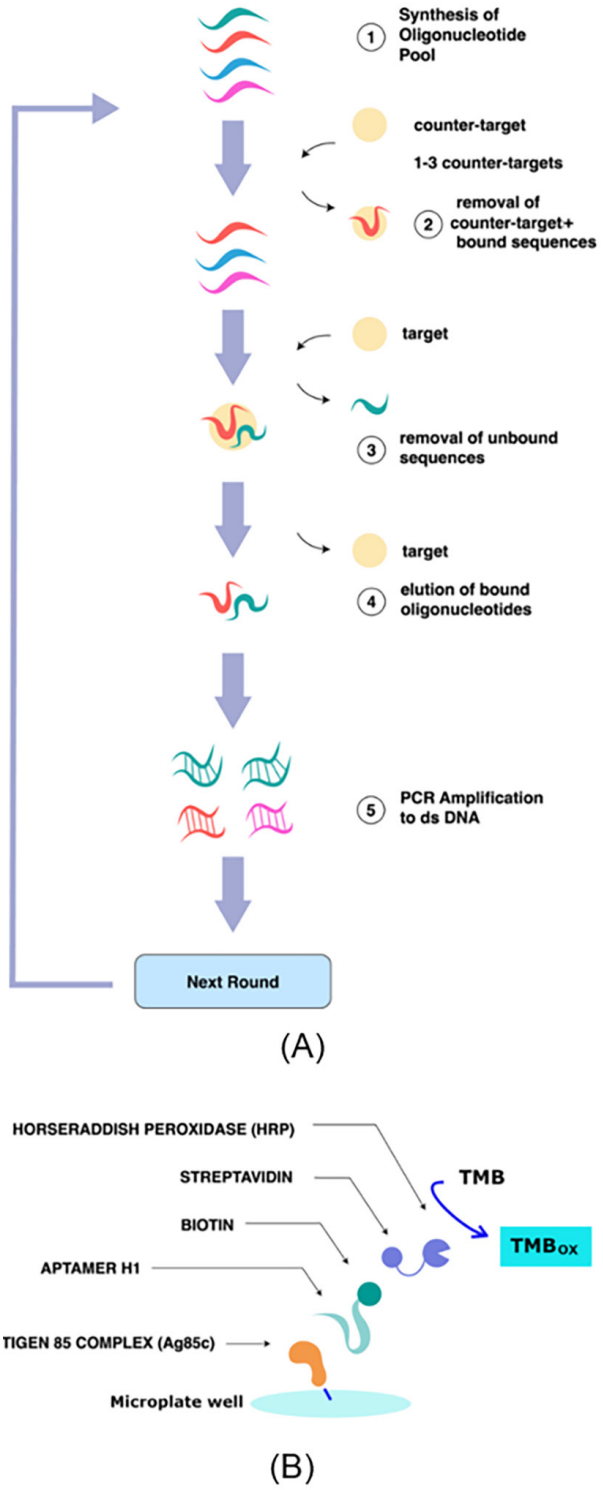

Figure 1. [A] Illustration of the microplate-based systematic evolution of ligands by exponential enrichment (SELEX) process and [B] assembly of biomaterials in enzyme-linked oligonucleotide assay (ELONA).

via the asymmetric PCR method, followed by digestion with lambda exonuclease. The double-stranded DNA and the regenerated oligonucleotide pool were cleansed using purification kits. The regenerated oligonucleotide pool was then used for the next SELEX rounds. Agarose gel electrophoresis was performed to check the recovery and evolution of aptamers after each SELEX round. After the eighth SELEX round, aptamer evolution was apparent. The aptamer pool from the last round was then sent to the University of the Philippines–Philippine Genome Center (UP-PGC) DNA Core Sequencing Facility to perform capillary electrophoresis Sequencing to identify the dominant aptamer sequence. The dominant aptamer sequence was named aptamer H1. A known aptamer sequence named aptamer H2 (an aptamer candidate for *M. tb.* ESAT-6 antigen) was selected as an aptamer candidate with parallel tests performed with aptamer H1. Aptamer candidates H1 and H2 have significant structural differences, as shown in Figures 3B and 3C.

Enzyme-linked Oligonucleotide Assay (ELONA)

Aptamer candidates were screened based on their binding affinity and specificity. Direct ELONA is illustrated in Figure 1B. Direct ELONA was performed based on the conventional ELISA technique to determine the aptamer-antigen complex formation's dissociation constant (K_d). A low nanomolar K_d indicates an effective binding affinity of a candidate aptamer. Specificity was also assessed using direct ELONA by determining each candidate aptamer's possible cross-reactivity with the other *M. tb.* antigens.

Various concentrations of the aptamer candidates were initially prepared starting at 1 µM. In a microtiter plate, 50 µL of 20 µg/mL Ag85c antigen was immobilized overnight at room temperature for each prepared aptamer dilution. Additional wells were allotted for blank testing. This was followed by blocking each well with PBS-Tween 20 for 1 h at room temperature and washing with the same solution. The initially prepared biotinylated candidate aptamers were added to each well and incubated for 30 min at room temperature. After incubation, the aptamer solution was removed, and each well was washed thrice with SELEX buffer. In each well, 50 µL of 50 ng/mL of HRP-streptavidin solution was added and was incubated at 37 °C for 30 min. The fluid was then removed, and the wells were washed with PBS buffer thrice. Next to washing, 50 µL of TMB solution was added, and after 10 min (blue color development is apparent), 50 µL of 1 M sulfuric acid solution was added to stop the reaction. The absorbance was then measured at 450 nm using a microplate absorbance reader (iMark, Bio-RAD, CA, USA).

The antigens Ag85c, LpqH, Ag85A, and ESAT6 were immobilized overnight at room temperature in separate microplate wells for cross-reactivity testing. Direct ELONA was performed using the previously described procedure, with the aptamers prepared at 100 nM and 1 µM concentrations.

Surface Plasmon Resonance (SPR)

Aptamer candidates H1 and H2 were sent to the UP-PGC Protein, Proteomics, and Metabolomics Facility (PPMF) to perform SPR, which was used to study the binding kinetics and affinity of each aptamer candidate with the antigen using Biacore X100 and Sensor Chip CM5. The SPR evaluation was performed based on the Langmuir fitting model (1:1 binding), as shown below:

$$A + B \underset{k_d}{\overset{k_a}{\rightleftharpoons}} B_A$$

$$K_D = \frac{k_d}{k_a}$$

Data Interpretation

Python scripts were created to generate graphs, perform four-parameter logistic regression (4PL), calculate the apparent dissociation constant (K_d) based on EC_{50}, and perform statistical analyses.

RESULTS

Sequence and Aptamer Structure Prediction

Agarose gel electrophoresis was used to monitor the recovery of the oligonucleotide pool from each SELEX round and assess the enrichment process. The amount of oligonucleotide recovered increases as specific sequences are enriched. The aptamer pool obtained from the last SELEX round was sent to the UP-PGC DNA core sequencing facility to perform capillary electrophoresis sequencing (Sanger sequencing). The chromatogram is shown in Figure 2. The chromatogram showed the detection of the primer sequences. The sequence in the random region is now apparent and denoted as aptamer H1. A non-specific aptamer to Ag85c, aptamer H2, obtained from another SELEX as a candidate aptamer for ESAT6, was also tested in parallel with aptamer H1 testing as a non-specific aptamer control. The secondary structure of H1 and H2 were predicted using Mfold (DNA folding form) (Zuker 2003), and the 3D structure was generated using RNA composer (Popenda *et al.* 2012; Sarzynska *et al.* 2023). Figure 3 shows the structure of the *M.Tb.* Ag85 complex and aptamer H1 have a stem-loop shape and the hairpin at the end, whereas aptamer H2 has hairpin

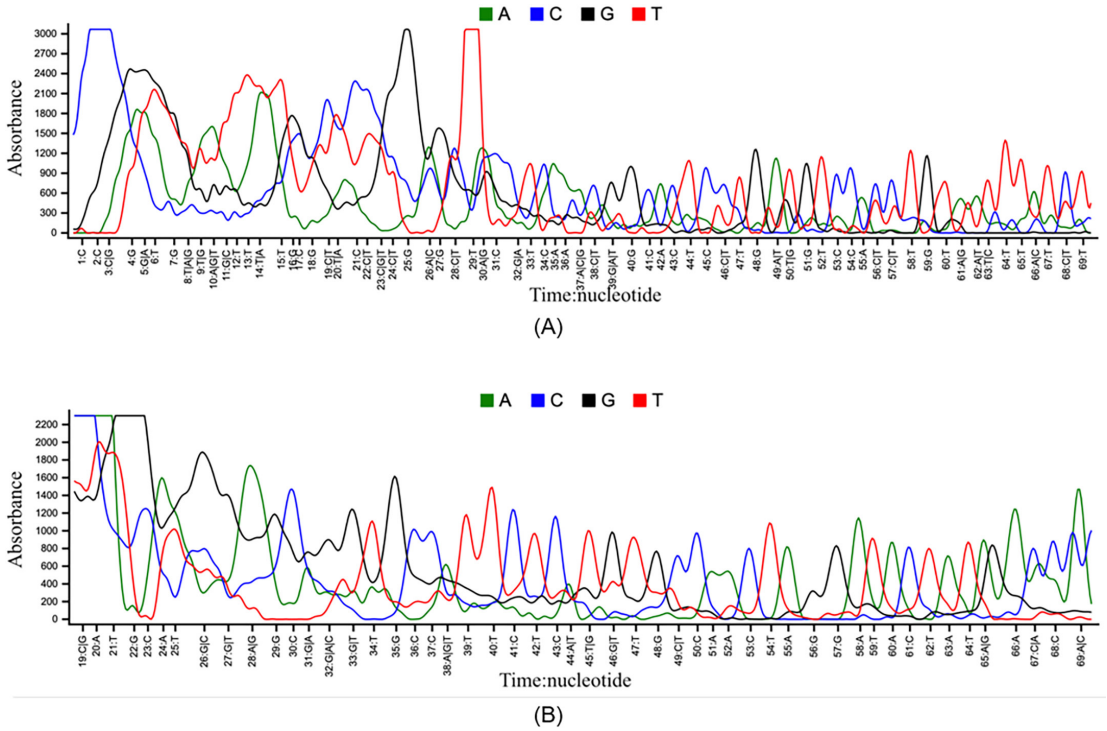

Figure 2. Capillary electrophoresis (Sanger) sequencing chromatogram results with the interpreted nucleotide sequence: [A] 5'-CCC-GGT-GTT-AGT-TTT-GCG-CTC-CCC-GAG-CTA-CGT-CAA-ACG-GCA-CTC-CTG-ATG-TCC-ACC-TGT-AAT-TTA-TCT-TCT-GGA-GCT-AAG-ATA-3', the reverse complement 5'- TAT-CTT-AGC-TCC-AGA-AGA-TAA-ATT-ACA-GGT-GGA-CAT-CAG-GAG-TGC-CGT-TTG-ACG-TAG-CTC-GGG-GAG-CGC-AAA-ACT-AAC-ACC-GGG-3', and [B] 5'-CCT-NGC-NGA-GTA-TGA-CGT-CAT-GCA-TGG-AGC-GGG-TGC-ATT-CTC-ATG-TGC-CAA-CTA-GGA-TAC-TAT-AAC-CAC-AAA-3' using reverse and forward primer as templates, respectively. Capillary electrophoresis (Sanger) sequencing was performed in UP PGC, Quezon City, the Philippines. Graph and sequences were generated using the Teal web application (https://www.gear-genomics.com/teal/).

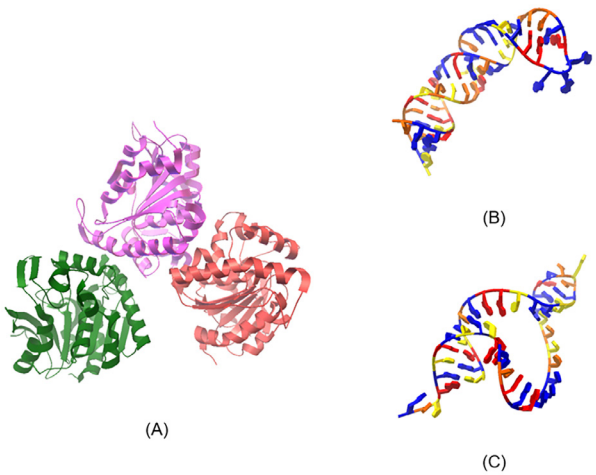

Figure 3. [A] *Mycobacterium tuberculosis* antigen 85 complex composed of FbpA with a sequence length of 304 bp, FbpB with a sequence length of 325 bp, and FbpC with a sequence length of 280 bp, obtained from the public repository RCSB Protein Data Bank (https://www.rcsb.org). [B] Identified sequences (length equals 50 bp) for aptamer candidate H1 and [C] aptamer candidate H2 with 3D structure generated using RNA composer (https://rnacomposer.cs.put.poznan.pl) (Popenda *et al.* 2012; Sarzynska *et al.* 2023). 3D structures are not drawn to scale.

structures along its strand, providing a broader aptamer coverage. Both aptamers were synthesized with biotin labeled at its 5' end.

Binding Affinity Studies on Aptamer Candidates

Direct ELONA assessed the interaction between the aptamer candidates against the target Ag85c. The complex formation was characterized quantitatively by titrating the immobilized antigen with the biotinylated aptamer until saturation. The absorbances were plotted as a function of the titrant concentration, as shown in Figure 4. The half maximum effective saturation concentration (EC_{50}) shown in each curve equals the apparent dissociation constant (K_d). Using the 4PL model, the dissociation constant K_d was calculated as 2.72 pM and 0.38 nM for candidate aptamers H1 and H2, respectively. Candidate aptamer H1 has shown better binding affinity than candidate aptamer H2 based on these K_d. Candidate aptamer H1 also showed better specificity to the target (Figure 5), with a possibility of more favorable binding to Ag85A, one of the components of the Ag85 complex. Candidate aptamer H2 exhibited possible high binding affinity to the *M. tb.* lipoprotein antigen LpqH, with possible cross-reactivity

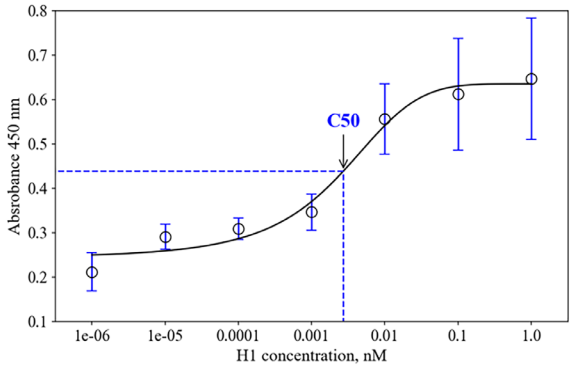

a = 0.2427, b = –4.6614, c = 2.5652, d = 0.6354 (R-sq = 0.9773)

[A]

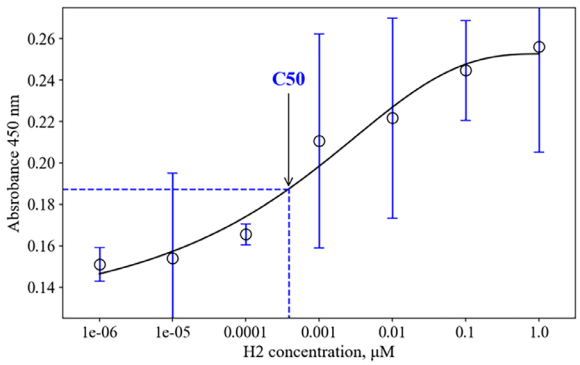

a = 0.1222, b = –2.6188, c = 3.4169, d = 0.2526 (R-sq = 0.9734)

[B]

Figure 4. *M. tb.* antigen 85 complex and aptamer candidate [A] H1and [B] H2 binding affinity study using ELONA with data points fitted to the 4-parameter logistic regression model (4PL), showing the half maximal effective concentration (C_{50}) to estimate the apparent dissociation constant of each aptamer candidate. Note the difference in binding performance between aptamer candidate H1 and H2, with H2 having a wider variance, resulting in a substantial standard error, as shown in Table 1.

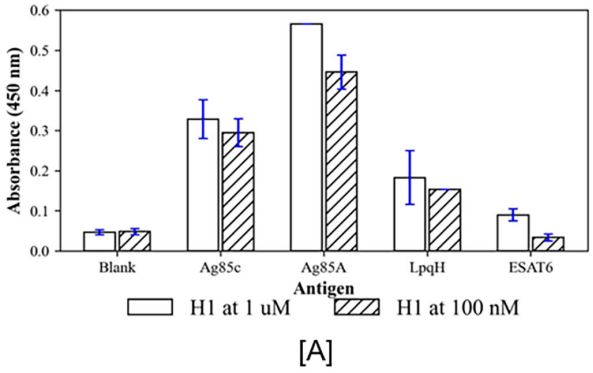

[A]

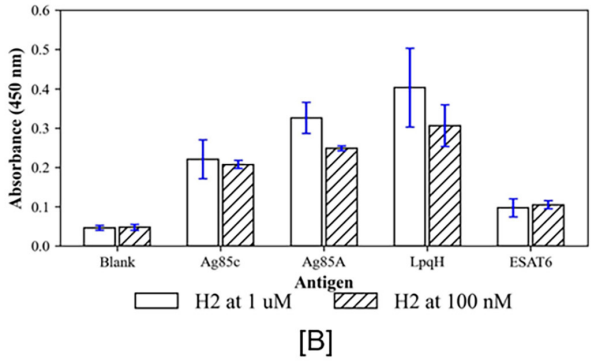

[B]

Figure 5. Aptamer candidate [A] H1and [B] H2 cross-reactivity study with *M. tb.* antigens Ag85 complex (Ag85A, Ag85B, and Ag85C), Ag85A, LpqH, and ESAT-6. Aptamer candidate H1 shows high affinity with the Ag85A component of the Ag85 complex, whereas aptamer candidate H2 shows high affinity to LpqH with possible cross-reactivity with Ag85A.

with Ag85A. Both affinity and specificity are essential parameters used to evaluate the candidate aptamers.

The binding kinetics of both aptamer candidates were studied using SPR. The SPR setup and the resulting sensogram are shown in Figures 6A–B. Aptamer H1 binding kinetics provide a more conclusive and accurate result than H2. The dissociation constant obtained using ELONA and SPR is summarized in Table 1. A low nanomolar dissociation constant indicates high binding affinity and would result in a more sensitive detection device, whereas specificity will increase the detection accuracy.

Table 1. Comparison of dissociation constants obtained using ELONA and SPR.

Aptamer	ELONA, apparent K_d in nM (based on EC_{50})	± % standard deviation (± %SD)	SPR, binding kinetics K_d in nM (based on 1:1 binding)	Standard error (± SE)	U-value[a]
H1	0.00272	9.66	20.93	12.00	12
H2	0.383	30.18	Tested (no binding)	N/A	95

[a]A U-value < 15 is statistically optimal for SPR

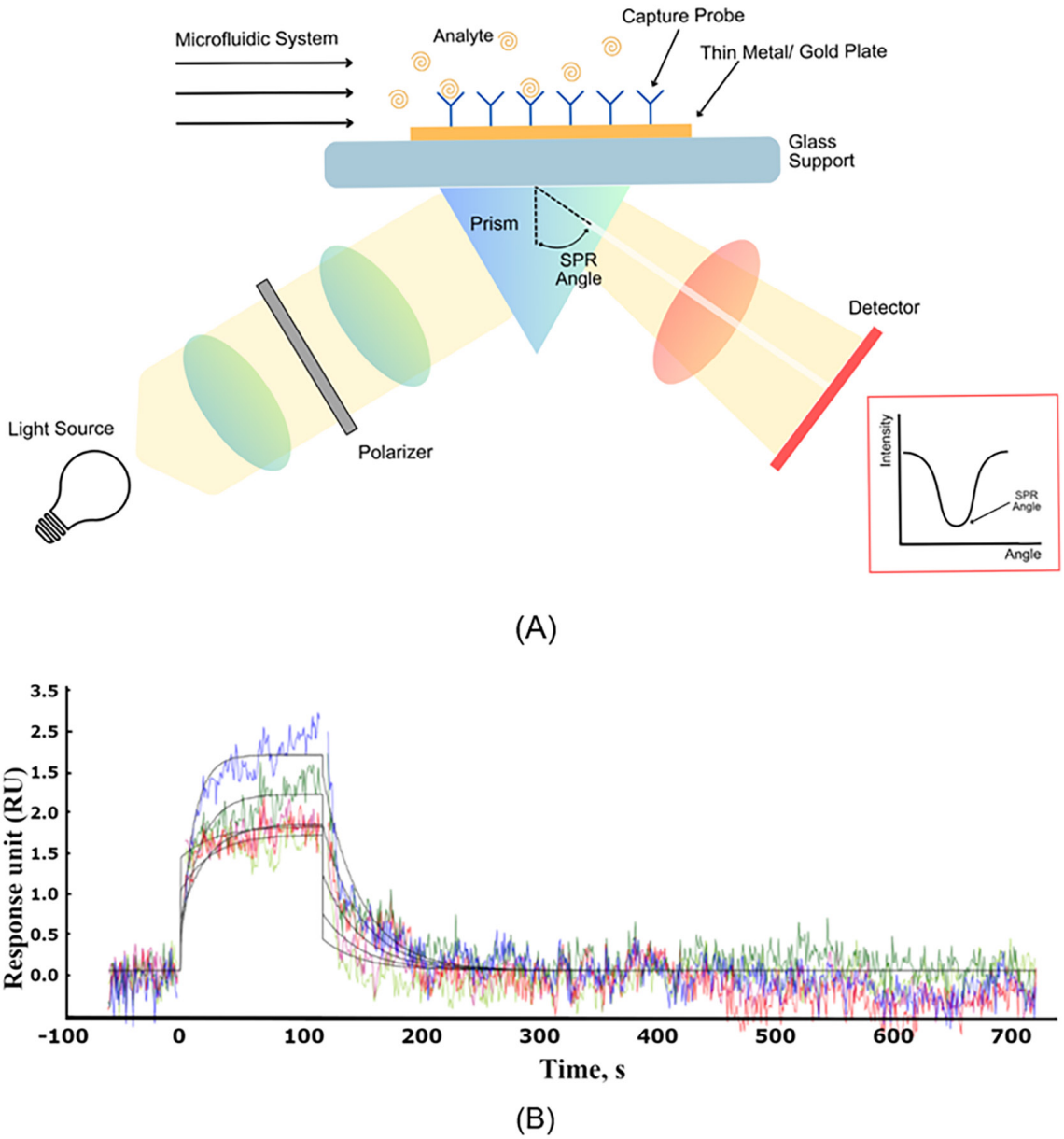

Figure 6. [A] Experimental set-up of the surface plasmon resonance (SPR) with the *M. tb.* antigen 85 complex immobilized on the Biacore™ CM5 sensor chip and aptamer candidate H1 as the analyte. [B] The sensogram of the binding kinetics study of aptamer candidate H1 using surface plasmon resonance (Biacore™ X100, UP PGC, Quezon City, the Philippines).

Table 2. Literature review of available aptamers against other TB antigens, with the SELEX process, binding test, and calculated dissociation constant.

***M. tb.* antigen**	**SELEX method**	**Binding test used**	**Dissociation equilibrium constant K_D, nM**	**Source**
IFN-γ	Beads-based SELEX	Flow cytometry	74.5	Cao *et al.* (2014)
MPT64	Membrane-based SELEX	SPR	8.92	Sypabekova *et al.* (2017)
ManLAM	Microplate-based SELEX	ELONA	668	Tang *et al.* (2016)
Ag85A	Beads-based SELEX	Flow cytometry	63	Ansari *et al.* (2018)
Ag85 complex	Microplate-based SELEX	SPR	20.93	This study

DISCUSSION

The SELEX process varies based on the partitioning technique used to separate the unbound and recover the bound aptamers. Protein-SELEX requires the target to be adsorbed passively or covalently on support platforms. The immobilization of the recombinant protein or antigens in a high-binding microplate for aptamer selection was confirmed by using the ELISA technique. The conventional SELEX process was slightly modified by incorporating a counter-target selection for each round of SELEX. In this process, the oligonucleotide library was first incubated against counter-target antigens before the target biomarker Ag85c. This resulted in highly specific aptamers compared to the candidate aptamers with similar binding affinity to Ag85c. It is crucial to monitor the enrichment of aptamer pools from each SELEX round to determine the progress of SELEX and to control the formation of mutated sequences.

Sanger sequencing has been used in many SELEX studies. However, current SELEX studies often employ the high throughput next-generation sequencing (NGS) that can produce millions of clone sequences in one run. The main objective of using Sanger sequencing is to obtain the overrepresented sequence. After the sixth SELEX cycle, a clone with a 22% count can be obtained using NGS (Schütze *et al.* 2011). The overrepresented sequence is the most abundant and assumed to be enriched after each SELEX cycle, which is strongly associated with the target. Sanger sequencing is not new to this application. However, obtaining more clones and sequences to choose from would be better, as they can only be provided by NGS. Some portion or nucleotides of the sequence were assumed; however, the generated 3D structure of the aptamer was used to justify such assumptions.

Sanger sequencing was used to generate highly accurate sequence data, particularly for short reads. However, this process is limited in its throughput compared to NGS, which can provide a large amount of sequencing data for in-depth analysis and optimization (Riley *et al.* 2015). In this study, the aptamer sequence obtained from Sanger sequencing met the objectives of high binding and highly specific candidate aptamer. The process can be improved further by applying NGS and *in silico* techniques to analyze the impact of different aptamer structural conformations.

The aptamer sequence was identified and purchased without the primer with biotin at its 5' end. The constant region or the primer-binding region is common to all sequences in the library, particularly used for PCR amplification. The aptamer library was designed so that this region will not affect the folding of the aptamer. In this study, the aptamer library comprises a constant region of 23-nt from 5' and 3' ends, with a 50-nt random region in the middle. A longer random region minimizes the influence of the constant region (primer region) on the aptamer structure. In theory, when the length of the random region is equal to or below 30 nt, the primer region would significantly impact the aptamer structure and influence its binding capabilities (Kohlberger and Gadermaier 2022).

ELONA was used to determine the K_d of each candidate aptamer and assess its cross-reactivity with the counter-target antigens. The result of ELONA is expected to vary depending on the reagents and equipment used. The four-parameter logistic regression model is commonly used to analyze the results of binding studies of bioassays such as ELISA. The curve fitting using this model was performed using the least squares methodology using a Python script. The half maximal effective concentration (EC_{50}), representative of the relative or apparent K_d, was obtained for the two candidate aptamers. The application of ELONA and the calculation procedure have effectively compared the binding performance of the two candidate aptamers. The result of the SPR binding kinetics study is strong evidence of the excellent performance of the aptamer H1. SPR is the gold standard used in studying the binding kinetics of biological molecules using a carboxyl-based or gold-based chip. Compared to ELISA or ELONA, SPR provides fast, reliable, and accurate results.

The SPR setup shown in Figure 6A includes the light source, the prism, the thin metal/gold plate, and the detector. The monochromatic light source is polarized to ensure that the electric field component is parallel to the metal surface to maximize the excitation of surface plasmons. The incident light is directed through the prism, coupling the light to the surface plasmons at the metal interface. A change in the refractive index near the metal plate indicates the binding of the molecules to the surface, shifting the angle at which the SPR occurs. The detector measures the intensity of the reflected light and analyzes the shift in the SPR angle to determine and quantify the extent of molecular binding (Nguyen *et al.* 2015).

The binding affinity of the aptamer candidates was assessed using ELONA and SPR, represented by the dissociation constant, K_d. A low nanomolar dissociation constant indicates the high potential of developing a biosensing system using the aptamer to detect its target antigen. The K_d of aptamer H1 was determined to equal 0.00272 nM, whereas aptamer H2 showed a higher K_d with about 197.16% difference from H1. The gold standard, SPR, showed a K_D measurement equal to 20.93 nM for aptamer H1, whereas K_D cannot be measured for aptamer H2 using the same technique due to its low binding affinity. Aside from the binding affinity, the cross-reactivity of the aptamer was assessed to determine

the potential co-detection of other antigens. H1 showed no evidence of cross-reactivity with other TB antigens in this case.

CONCLUSION

A microplate-based SELEX process successfully isolated an aptamer with high binding affinity and specificity to TB Ag85c antigen. Capillary electrophoresis sequencing was used to identify the isolated sequences, which were synthesized in biotinylated form without the forward and reverse primers. The aptamer candidate from SELEX, denoted as H1, and aptamer candidate H2 from the database were screened based on their binding affinity and specificity. Aptamer H1 showed a lower nanomolar dissociation constant, indicating a higher affinity to its target than H2. At the same time, aptamer H1 showed no cross-reactivity with the other TB antigens. SPR binding kinetics showed that the aptamer H1 has substantial potential for developing bioassay for antigen-based TB diagnostics.

ACKNOWLEDGMENTS

All antigens used in this study were obtained through BEI Resources, NIAID, NIH.

The authors would like to acknowledge the following research laboratories for their technical support and services: the National Immunological Testing Laboratory, the National Institute of Molecular Biology and Biotechnology, and the PPMF of the UP-PGC.

The authors would like to acknowledge the funding support from the Department of Science and Technology–Philippine Council for Health Research and Development and UP Los Baños.

Ms. Halyanna Mae M. Luis digitally drew all process illustrations.

STATEMENT ON CONFLICT OF INTEREST

The authors declare no conflict of interest.

REFERENCES

ANSARI N, GHAZVINI K, RAMEZANI M, SHAHDORDIZADEH M, YAZDIAN-ROBATI R, ABNOUS K, TAGHDISI SM. 2018. Selection of DNA aptamers against *Mycobacterium tuberculosis* Ag85A and its application in a graphene oxide-based fluorometric assay. Microchimica Acta 185(1): 21.

BARBIER E, FOUCHET T, HARTMANN A, CAMBAU E, MOUGARI F, DUBOIS C, LUBETZKI M, ROCHELET M. 2023. Rapid electrochemical detection of *Mycobacterium tuberculosis* in sputum by measuring Ag85 activity with disposable carbon sensors. Talanta 253: 123927.

BEKMURZAYEVA A, SYPABEKOVA M, KANAYEVA D. 2013. Tuberculosis diagnosis using immunodominant, secreted antigens of *Mycobacterium tuberculosis*. Tuberculosis 93(4): 381–388.

BENTLEY-HIBBERT SI, QUAN X, NEWMAN T, HUYGEN K, GODFREY HP. 1999. Pathophysiology of antigen 85 in patients with active tuberculosis: antigen 85 circulates as complexes with fibronectin and immunoglobulin G. Infection and Immunity 67(2): 581–588.

BEZERRA G, CÓRDULA C, CAMPOS D, NASCIMENTO G, OLIVEIRA N, SEABRA MA, VISANI V, LUCAS S, LOPES I, SANTOS J, XAVIER F, BORBA M, MARTINS D, LIMA-FILHO J. 2019. Electrochemical aptasensor for the detection of HER2 in human serum to assist in the diagnosis of early-stage breast cancer. Analytical and Bioanalytical Chemistry 411(25): 6667–6676.

CAO B, HU Y, DUAN J, MA J, XU D, YANG X D. 2014. Aptamer for assay of intracellular interferon-gamma. PLoS One 9: e98214.

ESPIRITU CAL, JUSTO CAC, JAUSET-RUBIO M, SVOBODOVA M, BASHAMMAKH AS, ALYOUBI AO, RIVERA WL, ROLLON AP, O'SULLIVAN CK. 2018. Aptamer selection against a *Trichomonas vaginalis* adhesion protein for diagnostics applications. ACS Infectious Diseases 4(9): 1306–1315.

HUYGEN K. 2014. The immunodominant T-cell epitopes of the mycolyl-transferases of the antigen 85 complex of *M. tuberculosis*. Frontiers in Immunology, Vol. 5.

JAYASENA SD. 1999. Aptamers: an emerging class of molecules that rival antibodies in diagnostics. Clinical Chemistry 45(9): 1628–1650.

KOHLBERGER M, GADERMAIER G. 2022. SELEX: critical factors and optimization strategies for successful aptamer selection. Biotechnology and Applied Biochemistry 69(5): 1771–1792.

KRISHNANANTHASIVAM S, LI H, BOUZEYEN R, SHUNMUGANATHAN B, PURUSHOTORMAN K, LIAO X, DU F, FRIIS CGK, CRAWSHAY-WILLIAMS F, BOON LH, XINLEI Q, CHAN CEZ, SOBOTA R, KOZMA M, BARCELLI V, WANG G,

HUANG H, FLOTO A, BIFANI P, … MACARY PA. 2023. An anti-LpqH human monoclonal antibody from an asymptomatic individual mediates protection against *Mycobacterium tuberculosis*. NPJ Vaccines 8(1): 127.

McKEAGUE M, CALZADA V, CERCHIA L, DEROSA M, HEEMSTRA JM, JANJIC N, JOHNSON PE, KRAUS L, LIMSON J, MAYER G, NILSEN-HAMILTON M, PORCIANI D, SHARMA TK, SUESS B, TANNER JA, SHIGDAR S. 2022. The minimum aptamer publication standards (MAPS guidelines) for *de novo* aptamer selection. Aptamer 6:10–18.

NGUYEN HH, PARK J, KANG S, KIM M. 2015. Surface plasmon resonance: a versatile technique for biosensor applications. Sensors 15(5): 10481–10510.

PHUNPAE P, CHANWONG S, TAYAPIWATANA C, APIRATMATEEKUL N, MAKEUDOM A, KASINRERK W. 2014. Rapid diagnosis of tuberculosis by identification of antigen 85 in mycobacterial culture system. Diagnostic Microbiology and Infectious Disease 78(3): 242–248.

POPENDA M, SZACHNIUK M, ANTCZAK M, PURZYCKA KJ, LUKASIAK P, BARTOL N, BLAZEWICZ J, ADAMIAK RW. 2012. Automated 3D structure composition for large RNAs. Nucleic Acids Research 40(14): e112–e112.

REAÑO RL, ESCOBAR EC. 2024. A review of antibody, aptamer, and nanomaterials synergistic systems for an amplified electrochemical signal. Frontiers in Bioengineering and Biotechnology 12: 1361469.

RILEY KR, GAGLIANO J, XIAO J, LIBBY K, SAITO S, YU G, CUBICCIOTTI R, MACOSKO J, COLYER CL, GUTHOLD M, BONIN K. 2015. Combining capillary electrophoresis and next-generation sequencing for aptamer selection. Analytical and Bioanalytical Chemistry 407(6): 1527–1532.

SAMANICH KM, KEEN MA, VISSA VD, HARDER JD, SPENCER JS, BELISLE JT, ZOLLA-PAZNER S, LAAL S. 2000. Serodiagnostic potential of culture filtrate antigens of *Mycobacterium tuberculosis*. Clinical Diagnostic Laboratory Immunology 7(4): 662–668.

SARZYNSKA J, POPENDA M, ANTCZAK M, SZACHNIUK M. 2023. RNA tertiary structure prediction using RNAComposer in CASP15. Proteins: Structure, Function, and Bioinformatics.

SCHÜTZE T, WILHELM B, GREINER N, BRAUN H, PETER F, MÖRL M, ERDMANN VA, LEHRACH H, KONTHUR Z, MENGER M, ARNDT PF, GLÖKLER J. 2011. Probing the SELEX process with next-generation sequencing. PLoS ONE 6(12): e29604.

SHOLA DAVID M, KANAYEVA D. 2022. Enzyme linked oligonucleotide assay for the sensitive detection of SARS-CoV-2 variants. Frontiers in Cellular and Infection Microbiology, Vol. 12.

SYPABEKOVA M, BEKMURZAYEVA A, WANG R, LI Y, NOGUES C, KANAYEVA D. 2017. Selection, characterization, and application of DNA aptamers for detection of *Mycobacterium tuberculosis* secreted protein MPT64. Tuberculosis 104: 70–78.

TANG XL, ZHOU YX, WU SM, PAN Q, XIA B, ZHANG XL. 2016. CFP10 and ESAT6 aptamers as effective *Mycobacterial* antigen diagnostic reagents. Journal of Infection 69: 569–580.

TUCCI P, PORTELA M, CHETTO CR, GONZÁLEZ-SAPIENZA G, MARÍN M. 2020. Integrative proteomic and glycoproteomic profiling of *Mycobacterium tuberculosis* culture filtrate. PLoS ONE 15(3): e0221837.

ZUKER M. 2003. Mfold web server for nucleic acid folding and hybridization prediction. Nucleic Acids Research 31(13): 3406–3415.